Journal of Materials Chemistry A

RSC Publishing

PAPER

View Article Online
View Journal | View Issue

Cite this: J. Mater. Chem. A, 2013, 1, 9907

Effect of molecular weight of additives on the conductivity of PEDOT:PSS and efficiency for ITO-free organic solar cells†

Desalegn Alemu Mengistie,[abc] Pen-Cheng Wang[c] and Chih-Wei Chu*[bd]

Received 2nd May 2013
Accepted 13th June 2013

DOI: 10.1039/c3ta11726j

www.rsc.org/MaterialsA

We systematically investigated the effect of the molecular weight of additives on the conductivity of poly(3,4-ethylenedioxythiophene):poly(styrene sulfonate) (PEDOT:PSS) by using different concentrations and molecular weights of polyethylene glycol (PEG) and ethylene glycol (EG). The conductivity enhancement depends on both the molecular weight and concentration of PEG used. The conductivity of PEDOT:PSS was enhanced from 0.3 S cm^{-1} to 805 S cm^{-1} with 2% PEG but to only 640 S cm^{-1} with 6% EG. PEGs with molecular weight higher than 400 have too low mobility to impart the required screening effect, and hence, the conductivity enhancement is less. Through FTIR, XPS and AFM investigations, the mechanism for the conductivity enhancement is found to be charge screening between PEDOT and PSS followed by phase separation and reorientation of PEDOT chains leading to bigger and better connected particles. The molecular weight and concentration of PEG also affect solar cell performances even though the conductivities are the same. Due to their high conductivity and high transmittance, ITO-free organic solar cell devices fabricated using PEDOT:PSS treated with 2% PEG anodes exhibited performance almost equal to that of the ITO counterparts.

1 Introduction

Organic solar cells (OSCs) which use either small molecules or polymers as active solar harvesting materials with promising potential for roll-to-roll and large area processing, flexibility and cheap cost of manufacture are considered as next generation green energy sources.[1–3] A better understanding of the mechanism facilitated a rapid increase in power conversion efficiency and the recently reported efficiency of 12% is paving the way for their commercialization.[4–6] The next technical challenge is to realize the high speed manufacturing of cells and modules with long lifetimes. OSCs contain bottom and top electrodes, interlayer materials and active layer materials. As the interlayer and active layer materials can be processed through conventional solution processing, the electrodes which are deposited through vacuum deposition are the bottleneck for the roll-to-roll high speed processing of OSCs. At least one of the electrodes in opto-electronic devices needs to be transparent in order to allow light to be harvested by the active layer or to emit light. However, tin doped indium oxide (ITO) coated on rigid glass which is currently used as the standard transparent electrode has many drawbacks. ITO's price is skyrocketing due to its limited availability; moreover, ITO is mechanically brittle and exhibits poor adhesion to organic and polymeric materials.[7,8] In OSCs, 37–50% of the material cost is from ITO.[1] Moreover, ITO has additional inherent problems such as release of oxygen and indium into the organic layer, poor transparency in the blue region, and complete crystallization of ITO films, which requires high temperature processing.[9] Hence, ITO is a non-ideal transparent electrode for opto-electronic devices and a search for an alternative transparent electrode is inevitable.[10]

Different materials including metal nanowires,[11–13] carbon nanotubes,[14–16] graphene[17–19] and conducting polymers[20–24] are being actively investigated as replacements for ITO. Among them, the conductive polymer poly(3,4-ethylene dioxythiophene) (PEDOT) doped with poly(styrene sulfonate) (PSS) (chemical structure shown in Fig. 1a) is quite promising as a next-generation transparent electrode material owing to its enormous advantages over other conducting polymers. PEDOT is insoluble in most solvents but can be dispersed in water by using PSS as a counter ion, which also serves as an excellent oxidizing agent, as a charge compensator, and as a template for polymerization.[25,26] PEDOT:PSS films have high transparency in the visible range, high mechanical flexibility, and excellent

[a]Nanoscience and Technology Program, Taiwan International Graduate Program, Academia Sinica, Taipei 115, Taiwan

[b]Research Center for Applied Sciences, Academia Sinica, Taipei 115, Taiwan. E-mail: gchu@gate.sinica.edu.tw; Fax: +886-2-27896680; Tel: +886-2-27898000 ext. 70

[c]Department of Engineering and Systems Science, National Tsing Hua University, Hsinchu 30013, Taiwan

[d]Department of Photonics, National Chiao Tung University, Hsinchu 300, Taiwan

† Electronic supplementary information (ESI) available: PEDOT:PSS film after PEG400 and methanol treatment, XPS spectra of PEDOT:PSS with PEG400 and *J–V* curves and device performance tables of OSCs with PEDOT:PSS anodes treated with different concentrations of PEG. See DOI: 10.1039/c3ta11726j

thermal stability and can be fabricated through conventional solution processing. PEDOT:PSS films can also be easily nanostructured to enhance the localized light intensity to the active layer and generate more power.[27] Different grades of PEDOT:PSS dispersions with different conductivities are commercially available for antistatic coating, hole injection layer and transparent electrode applications. However, pristine PEDOT:PSS films suffer from a very low conductivity of less than 1 S cm^{-1}, which is quite low to be used as standalone electrodes.

Several methods are being actively investigated to enhance the conductivity of PEDOT:PSS by more than three orders of magnitude to replace ITO. The methods employed for conductivity enhancement of PEDOT:PSS including the treatment chemicals used have been recently reviewed by Po *et al.*[28] The approaches include the addition of organic compounds such as ethylene glycol (EG), dimethyl sulphoxide, dimethyl sulphate, sorbitol, mannitol, ionic liquids, and anionic surfactants into the PEDOT:PSS aqueous solution,[29–35] treatment of PEDOT:PSS films with polar organic compound, salt, acid, zwitterions or cosolvents[36–40] or a combination of both mixing the additive in the PEDOT:PSS dispersion and film treatment.[41] Xia *et al.* enhanced the conductivity of Clevios PH1000 PEDOT:PSS to 3065 S cm^{-1} by treating the film three times with 1 M sulphuric acid at 160 °C.[42] Fabretto *et al.* also reported PEDOT films with a conductivity of 3400 S cm^{-1} using vacuum vapour phase polymerization technique.[43] But the performances of the OSC devices fabricated with these high conductivity PEDOT:PSS anodes were lower than the ITO counterparts. In addition to high conductivity, high transmittance and other film properties should not be impaired during film treatment.

Even though such high conductivities are obtained, the fundamental mechanisms of conductivity enhancement are not well understood yet. It has been said that the origin and mechanism of conductivity improvement differ widely and are considered controversial.[29,44,45] In our earlier report,[46] we showed that the mechanism of conductivity enhancement depends on the treatment chemical, its properties and the method of treatment employed and some of the mechanisms proposed are complementary. We used methanol, which previously was considered as not to significantly enhance conductivity, to treat PEDOT:PSS films and the conductivity was enhanced to 1362 S cm^{-1}. Morphology changes with phase separated PEDOT and PSS leading to larger grain sizes and lower intergrain hopping,[30,47] screening effect by polar solvents,[48] washing away of the excess insulator PSS from the film surface,[41,46] conformational changes by reorientation of PEDOT:PSS chains leading to better connection between the conducting PEDOT chains,[45] and even some doping effects are among the mechanisms proposed by different researchers.[33,42] Takano *et al.* used small- and wide-angle X-ray scatterings and found that nanocrystals of PEDOT are formed.[49] Polar solvents which are secondary dopants added in the PEDOT:PSS aqueous solution bring about morphology changes showing larger grain size and better connected PEDOT chains, whereas those film treatments lead to both morphology change and removal of excess PSS from the film surface. Owing to this, mostly methods employing film treatment or both film treatment and additives in the solution show better conductivity than the mere additives in the PEDOT:PSS aqueous solution.[41,42,46]

In this study, we showed the effect of the molecular weight/chain length of the additive on the conductivity and other properties of PH1000 PEDOT:PSS films using EG and different molecular weight polyethylene glycols (PEGs). While the conductivity of PEDOT:PSS increases with increasing EG concentration and saturates at 6% addition, the conductivity reaches saturation at 2% PEG concentration and even decreases afterwards. The average conductivity was significantly enhanced from 0.3 S cm^{-1} to 805 S cm^{-1} with PEGs having molecular weights from 200 to 400 but to only to 640 S cm^{-1} with 6% EG. Even though PEGs with molecular weight higher than 600 still bring about conductivity enhancement, the conductivity is less than that obtained using EG. Phase separation between PEDOT and PSS chains facilitated by the additives leading to better connected and bigger PEDOT chains is the main reason for the conductivity enhancement. FTIR and XPS measurements revealed that PEG still remains in the films forming hydrogen bonding with PSS. ITO-free OSCs fabricated with PEG treated PEDOT:PSS films as standalone transparent electrodes demonstrate better than EG treated anodes and showed performance almost equal to that of the devices with ITO electrodes.

2 Experimental

2.1 Preparation and characterization of PEDOT:PSS films

PEDOT:PSS aqueous solution (Clevios PH1000) with a PEDOT:PSS concentration of 1.0–1.3% by weight was purchased from Heraeus Ltd. and the weight ratio of PSS to PEDOT is 2.5. Glass substrates with an area of 1.5 × 1.5 cm^2 were cleaned by sonication successively in detergent water and twice with deionized water for 15 min each time and then dried in an oven after purging with N_2 air. Different concentrations (v/v%) of EG and PEG were mixed with PEDOT:PSS aqueous solution. Different molecular weights of PEG were used (PEG200, PEG300, PEG400, PEG600, PEG1000 and PEG6000, the number indicating the molecular weight). PEDOT:PSS mixed with EG and PEG filtered through a 0.45 μm PTFE syringe filter was spin coated at 3000 rpm for 60 s on glass substrates which were treated with UV/ozone for 15 min prior to spin coating. The films were annealed on a hot plate under ambient atmosphere at 130 °C for 30 min. Thicker PEDOT:PSS films were prepared by spin coating multiple times and annealing after each layer. For some films, a combined treatment with methanol was performed by immersing the annealed films in methanol for 10 min and then the films were again dried at 140 °C for 5 min. The other combined film treatment was done by dropping 120 μL of methanol on the film at 130 °C after annealing for 5 min.

Film thickness was measured using a Veeco Dektak 150 alpha step surface profiler. Conductivities were measured using van der Pauw four-point probe technique with a Hall effect measurement system (Ecopia, HMS-5000). Transmission spectra of the films were measured using a Jacobs V-670 UV-Vis-NIR spectrophotometer. The transmittance values reported in this paper are at a wavelength of 550 nm and include the

absorption of the glass substrate. X-ray photoelectron spectroscopy (XPS) was performed using a PHI 5000 VersaProbe equipped with an Al Kα X-ray source (1486.6 eV). Attenuated total reflectance Fourier transform infrared (ATR-FTIR) spectroscopy was performed using an FT-IR spectrometer (PerkinElmer, Spectrum 100) for PEDOT:PSS films coated on glass or by dropping PEG solution on the IR cell. Veeco di Innova was used in the taping mode to take the atomic force microscopy (AFM) images of polymer films.

2.2 Fabrication and characterization of OSCs

OSCs were fabricated using both ITO-free highly conductive EG and PEG treated PEDOT:PSS films and ITO (<7 Ω $\square^{-1}$, RiT display) anodes on glass. A relatively well studied and stabilized donor:acceptor blend of poly(3-hexylthiophene) (P3HT) and [6,6]-phenyl-C_{61}-butyric acid methyl ester ($PC_{61}BM$) was used as the active layer. The OSC devices were fabricated by spin coating a blend solution of P3HT:PCBM, prepared by dissolving 20 mg mL^{-1} of each component in 1,2-dichlorobenzene at 70 °C for 3 h, at 600 rpm for 60 s in a nitrogen filled glove box on the PEDOT:PSS treated with EG and PEG and the ITO surface. Less conductive PEDOT:PSS (Clevios P VP 4083) was spin coated at 4000 rpm for 60 s on the ITO surface as a buffer layer and annealed in the same way prior to the active layer deposition. The active layer was then solvent annealed by covering in glass Petri dishes for 30 min, and subsequently, the films were annealed on top of a hotplate at 130 °C for 30 min. The devices were completed by thermal deposition of 30 and 60 nm thick calcium and aluminium, respectively, at a pressure below 10^{-6} Torr through a shadow mask.

The photovoltaic performance of the devices was measured inside a glove box filled with N_2 under simulated AM 1.5G illumination (100 W cm^{-2}) using a xenon lamp based solar simulator (Thermo Oriel 1000 W). The light intensity was calibrated by a mono-silicon photodiode with a KG-5 color filter (Hamamatsu, Inc.). Devices were illuminated under mask and the active area of the device was controlled to be 0.1 cm^2. The external quantum efficiency (EQE) spectra were obtained under short-circuit conditions. Devices were encapsulated before they were taken out for the EQE measurement. The light source was a 450 W Xe lamp (Oriel Instruments, Model 6123NS). The light output from the monochromator (Oriel Instruments, Model 74100) was focused on the photovoltaic cell being tested.

3 Results and discussion

3.1 Conductivity and opto-electronic properties of treated PEDOT:PSS films

It is well known that adding polyols in an aqueous solution of PEDOT:PSS or film treatment with them can significantly enhance its conductivity. The physical properties of the additives like hydrophilicity and dielectric constant affect the conductivity. However, there is no systematic study on the effect of the molecular weight/chain length of the additives on the conductivity and finally on the device performance especially when the additive is an oligomer or a polymer. Here, we studied

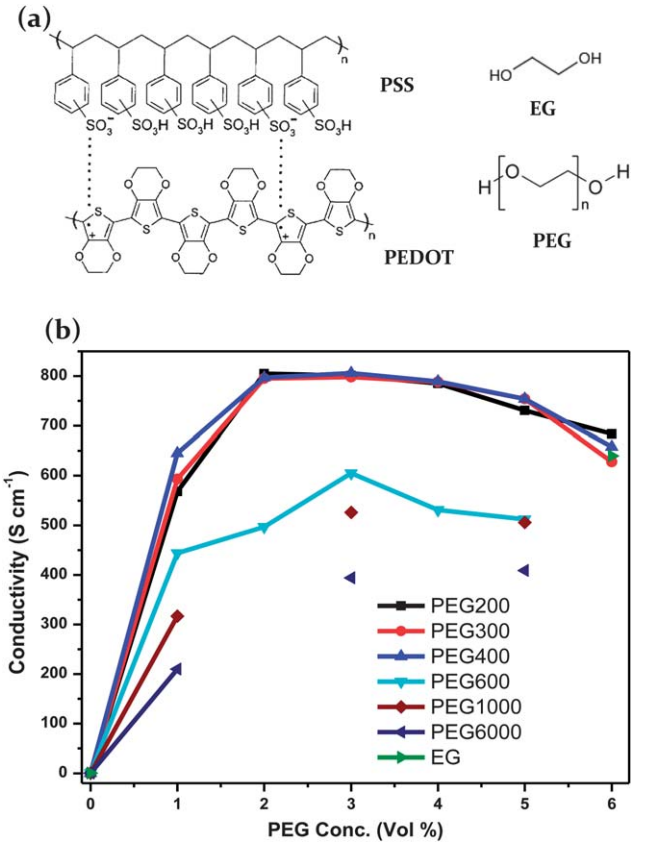

Fig. 1 (a) Chemical structures of PEDOT:PSS, EG and PEG. (b) Conductivities of PEDOT:PSS treated with different molecular weight PEGs with different concentrations.

systematically the effect of the additive molecular weight on the conductivity of PEDOT:PSS using EG and different molecular weight PEGs. Fig. 1 shows the conductivities of PH1000 PEDOT:PSS films prepared by using EG and different molecular weight PEGs with different concentrations. As PEG is a polymer of EG, conductivity enhancement is expected. PEGs with molecular weights 200, 300 and 400 showed almost the same conductivity and the average conductivity was tremendously improved from 0.3 S cm^{-1} to 805 S cm^{-1} using 2% PEG additive, and then it slightly decreased, whereas the conductivity was only 640 S cm^{-1} when 6% EG was used. PEGs with molecular weights of 600 and higher showed lower conductivity than EG, but the trend is similar to that of the other lower molecular weight PEGs. As reported elsewhere,[41] the conductivity increases gradually from 1% to 4% EG, reaches maximum at 6% EG and then levels off afterwards, whereas even the 1% PEG additive tremendously enhanced the conductivity. Wang *et al.* used PEG400, PEG800 and higher molecular weight PEGs to enhance the conductivity of PEDOT:PSS but the conductivity was enhanced to only 17.7 S cm^{-1} using PEG400,[50] even though they did not mention the grade of PEDOT:PSS used and also did not compare it with EG. They observed a similar conductivity enhancement trend with increasing concentration and molecular weight of PEG. We also noted that the viscosity of the PEDOT:PSS solution increased with increasing PEG

concentration and film uniformity was decreasing by shrinking at the edges especially for higher molecular weight PEGs. The decrease in conductivity with increasing PEG concentration may be attributed to the increase in the insulator PEG on the film surface as the high boiling point PEG will not evaporate during annealing.

In an effort to further enhance the conductivity, we applied film treatment either by dropping methanol on the film or immersing in methanol solution as reported in our previous work.[46] The conductivity was further enhanced to more than 1100 S cm^{-1} after methanol treatment by either method for EG and PEG200 treated films with all concentrations. Additionally, methanol treatment brought better film uniformity. For films prepared using 1% and 2% PEG300 additives, conductivity could be enhanced the same as EG and PEG200 by methanol treatment but for higher concentrations of the PEG300 film, it was disrupted by methanol. Methanol treatment disrupted all PEDOT:PSS films prepared with all concentrations of PEG400 and higher as shown in Fig. S1 (ESI†). Disruption of the PEDOT:PSS film with a higher molecular weight PEG indicates that both PEG and PSS have formed some kind of interaction and are removed by methanol as both are soluble in methanol.

The relationship between conductivity, mobility and bulk concentration is given by:[51]

$$\sigma = e\mu N$$

where σ is the conductivity, e is the elementary charge, μ is the carrier mobility and N is the bulk concentration. As measured by the Hall effect measurement system, the bulk concentration of PEDOT:PSS films increased from an order of 17 cm^{-3} to an order of 21 cm^{-3} after film treatment and mobility was of the same order varying between 1 and 9 $cm^2\ V^{-1}\ s^{-1}$ before and after treatment. Here, it is clear that the conductivity enhancement is due to an increase in carrier concentration in contrast to Ouyang *et al.*'s[23,52] claim that conductivity enhancement is due to the charge carrier mobility resulting from conformational changes of PEDOT chains. This carrier concentration is equal or even a little higher than that of ITO. The bulk concentration for semimetals is in the order of 18 to 21 cm^{-3} and that of metals more than the order of 22 cm^{-3}.

Fig. 2a shows the transmittance spectra of ITO and PEDOT:PSS films prepared using 6% EG and 2% PEGs. All PEDOT:PSS films have better transmittance than ITO; the transmittance of PEDOT:PSS films treated with 6% EG and 2% PEG200 is 93% at 550 nm but that of ITO is only 88% including the glass substrate. The lower transmittance of ITO than PEDOT:PSS films is well noticeable in the violet and blue regions of the spectrum. Film thickness increased with increasing PEG molecular weight as well as increasing the concentration of PEG added in the PEDOT:PSS solution. The thicknesses of PEDOT:PSS films were 70 nm with 6% EG and 95 nm with 2% PEG200. Fig. 2b shows the variation of film thickness, transmittance and sheet resistance with PEG200 concentration. The transmittance value is above 92% till 2% PEG200 concentration and then goes down with increasing concentration in line with the increase in film thickness from

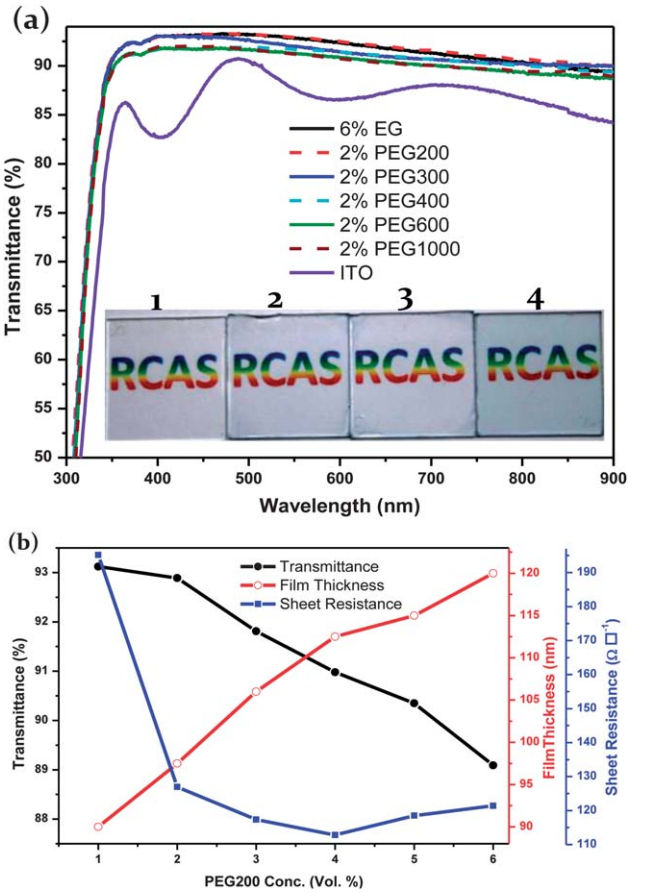

Fig. 2 (a) Transmittance spectra of ITO and PEDOT:PSS films treated with 6% EG and 2% PEGs. The inset compares the transmittances of bare glass (1), PEDOT:PSS treated with EG (2), PEG200 (3) and ITO (4). (b) Variation of transmittance, film thickness and sheet resistance with PEG200 concentration.

90 nm to 120 nm for 1% and 6% PEG200 concentrations, respectively. The sheet resistance decreased from 195 Ω $\square^{-1}$ to 113 Ω $\square^{-1}$ and then increased because of low conductivity. The sheet resistance can further be decreased by preparing multiple layers of PEDOT:PSS. Two layers of the PEDOT:PSS film fulfill the minimum optical and electrical requirements for transparent electrodes which are transmittance higher than 90% and sheet resistance less than 100 Ω $\square^{-1}$ ensuring that PEDOT:PSS films are promising replacements for ITO electrodes.

3.2 Mechanism of conductivity enhancement

To further explore the effect of PEG and the mechanism of conductivity enhancement, we utilized various chemical and physical characterizations. The FT-IR spectra of PEG400, PEDOT:PSS and PEDOT:PSS with 2% PEG400 are shown in Fig. 3. As the boiling point of PEG is more than 250 °C, it is expected that it will not evaporate by annealing at 130 °C for 30 min. The presence of the peaks at 2875 cm^{-1} (C–H stretching) and at 1645 cm^{-1} (C–O–H bending) both in PEG400 and in PEDOT:PSS films treated with PEG confirm the presence of PEG in the film. The FTIR spectra (not shown here) of PEDOT:PSS films treated with EG didn't show the presence of EG inside the film, which is in agreement with the previous reports.[23]

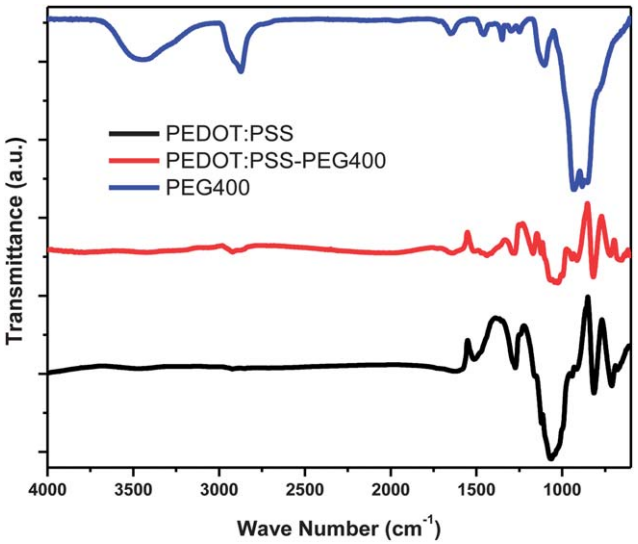

Fig. 3 ATR-FTIR spectra of PEDOT:PSS film, PEG400 solution and the PEDOT:PSS film treated with 2% PEG400.

Fig. 4 shows the XPS spectra of pristine PEDOT:PSS and those treated with 2% PEG and 6% EG. The S(2p) peak at the binding energy of 167.8 eV corresponds to the sulphur signal of PSS and those at 164 eV and 163 eV correspond to the sulphur signal of PEDOT (Fig. 4a).[53] The PEDOT:PSS ratio increased after treatment with EG and PEG which is due to the depletion of the PSS layer from the film surface. The PEDOT:PSS ratio of PEG200, 300 and 400 treated films is more than the one treated with EG, which is in agreement with the conductivity enhancement. PEG and EG induce a screening effect between the positively charged PEDOT chains and negatively charged PSS chains, thus reducing the coulombic interaction between them.[48] The reduction of the coulombic interaction between PEDOT and PSS chains facilitates phase separation on the nanometer scale. Eventually, by segregation of the excess PSS, there will be higher PEDOT domains on the film surface which leads to higher conductivity. The sulphur signal could not be detected from PEDOT:PSS films treated with PEG600 and 1000. The film should be covered with a thin layer of PEG. Longer chain PEG has low mobility and some chains will remain on the film which again is the reason for the low conductivity with higher molecular weight PEGs. The sulphur signal was also weak or films were covered with PEG400 beyond 2% concentration (Fig. S2, ESI†). The C(1s) and O(1s) core level spectra (Fig. 4b and c) of pristine and EG and PEG treated PEDOT:PSS are different. The C(1s) peak is at 283.6 eV for pristine and EG treated films but it is shifted to 285.4 eV for PEG treated PEDOT:PSS films.[54] PEDOT:PSS films with 2% PEG200 have a main peak at 283.6 eV and a small peak at 285.4 eV, indicating that only a small amount of PEG200 is present in the film. Films with 2% PEG300 show a main peak at 285.4 eV and a small peak at 283.6 eV. Pristine and EG treated PEDOT:PSS films have the same O(1s) spectra with a peak at 531 eV but it is shifted to 531.8 eV for PEG treated films. The shifting of the C(1s) and O(1s) peaks to higher energy for PEG treated PEDOT:PSS films confirms the presence of PEG in the film. As the boiling point of PEG is more than 250 °C, the presence of PEG in the PEDOT:PSS film will not affect its thermal stability.

Conductivity is also related to film morphology and the changes in film morphology before and after film treatment were investigated by taking AFM images (Fig. 5). The phase image is homogeneous with disconnected PEDOT chains and weak phase separation between PEDOT and PSS for the pristine films, whereas there is a good phase separation between PEDOT and PSS chains with more fiber like interconnected conductive PEDOT chains after film treatment with both EG and PEG. The

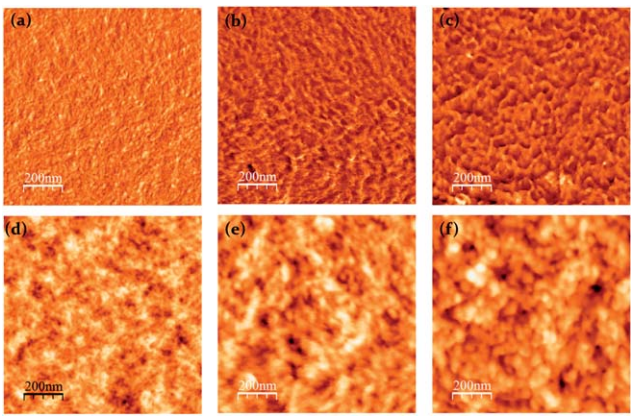

Fig. 5 AFM images of PEDOT:PSS films: pristine (a and d), treated with 6% EG (b and e) and treated with 2% PEG200 (c and f). (a), (b) and (c) are phase images, while (d), (e) and (f) are topographic images. All the images are 1 μm × 1 μm.

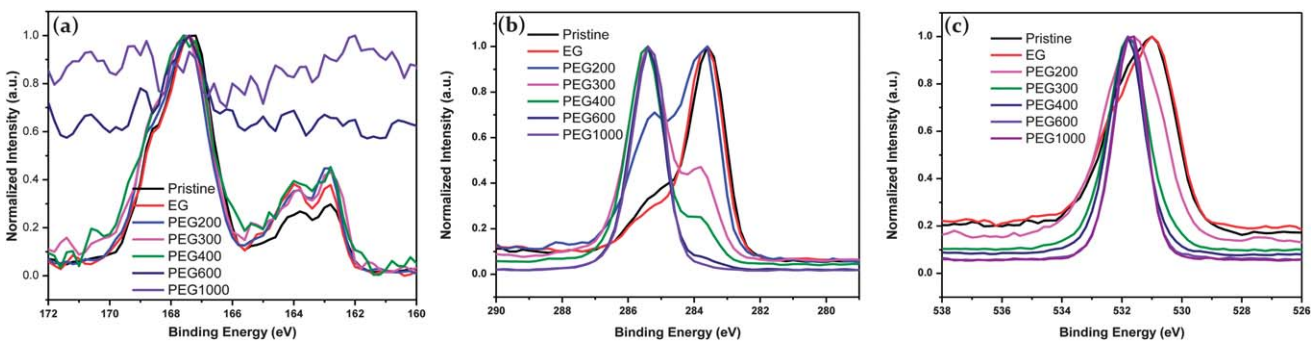

Fig. 4 XPS spectra of pristine PEDOT:PSS and PEDOT:PSS films treated with 6% EG and 2% PEG. (a) S(2p), (b) C(1s) and (c) O(1s) core-level spectra.

depletion of insulating PSS leads to a 3D conducting network of highly conductive PEDOT, resulting in an increase in the conductivity. The topographic AFM images indicate that bigger particles are formed after film treatment and those treated with PEG have a more elliptical shape which are bigger than those treated with EG. The rms roughnesses of the films are 1.2 nm, 1.35 nm and 1.46 nm for the pristine, 6% EG and 2% PEG200 treated PEDOT:PSS films, respectively. AFM images on films prepared with a higher molecular weight and a higher concentration of PEG are difficult to obtain because the films are covered with PEG; the same phenomenon was observed by Badre *et al.* when they used ionic liquids.[34] In these cases, the films were seen to be smoother than the pristine ones.

Xia and Ouyang[55] revealed that PEDOT:PSS with a higher average molecular weight of PEDOT chains will have bigger gel particles and increased conductivity after film treatment than the one with a low molecular weight. As particles grow, the total number of particle boundaries in a given volume or area decreases, and there will be few energy barriers for charge conduction.[47] Hence, charge hopping among the polymer chains which is believed to be the dominant conduction mechanism in conducting polymers will be easier.[56]

The fiber like phase separated interconnected PEDOT chains in the AFM phase images suggest that the conformation of PEDOT will be changed from a coiled to a linear/extended-coil structure owing to the depletion of PSS from the film surface. PEDOT and PSS are held by coulombic attractions and have a coiled or core–shell structure due to repulsion between long PSS chains.[57] The PEG/EG treatment screens the ionic interaction between PEDOT and PSS by forming hydrogen bonding with both PSS^- and PSSH. This will lead to better phase separation between PEDOT and PSS, linearly oriented PEDOT chains as proposed in Scheme 1 and bigger and more aggregated PEDOT chains on the film surface. Ouyang *et al.* also claimed that the EG treatment of PEDOT:PSS changes the resonant structure of PEDOT chains from a benzoid with a preferred coiled structure to a quinoid with a preferred linear or expanded-coil structure.[45] The reorientation of the PEDOT polymer chains from coiled to linear or extended-coil structure allows more inter-chain interaction between the conducting polymers; hence, the energy barrier for inter-chain and inter domain charge hopping will be lowered leading to better charge transfer among the PEDOT chains. PEDOT-rich chains with linear structure, larger grain size and lower intergrain hopping promote the charge hopping and eventually the conductivity is tremendously enhanced.

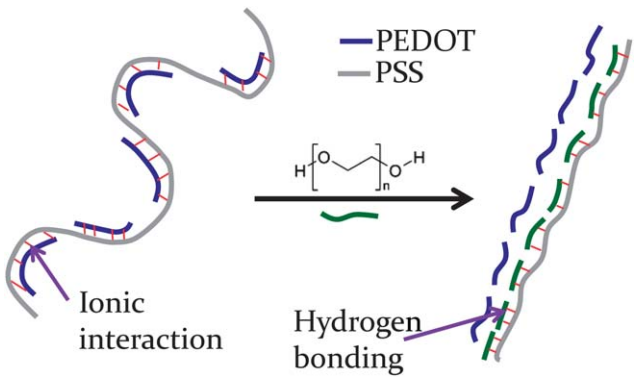

Scheme 1 Schematic illustration of the mechanism of conductivity enhancement of PEDOT:PSS with PEG.

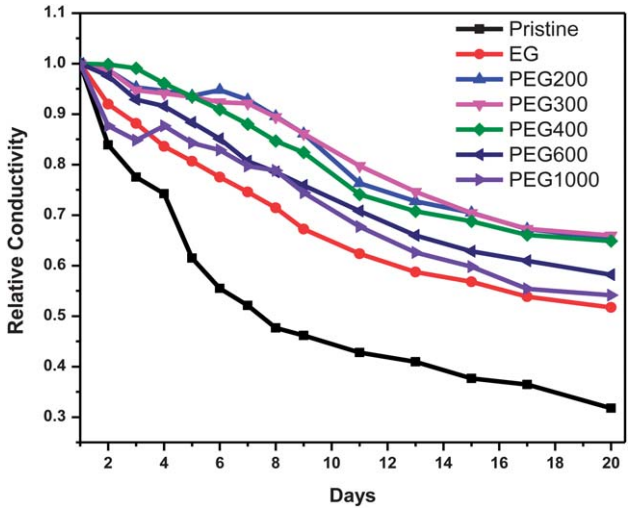

Fig. 6 Conductivity stabilities of pristine, 6% EG and 2% PEG treated PEDOT:PSS films in ambient atmosphere.

The depletion of the insulator hygroscopic PSS from the film surface will not only increase the conductivity of the film but will also improve its long term stability as PSS is the prime reason for the degradation of organic solar cells.[41,46] The conductivity stability of the PEDOT:PSS films was assessed by keeping them in ambient atmosphere at room temperature and humidity higher than 75%. PEDOT:PSS films treated with 2% PEG200, 300 and 400 maintained up to 66% of the original conductivity, while the film treated with 6% EG maintained 52% and the pristine film maintained only 32% in 20 days (Fig. 6). One reason for the conductivity loss through time is the absorption of moisture by hygroscopic PSS. As confirmed by FTIR and XPS measurements, PEG still remains in the film by forming hydrogen bonding with both PSS^- and PSSH. Hence, the tendency of the film to absorb moisture by forming hydrogen bonding will be less for films treated with PEG. For PEG600 and 1000, the conductivity loss is higher than the other PEGs due to the presence of PEG on the film surface which itself will absorb moisture.

3.3 ITO-free OSCs using PEDOT:PSS treated with PEG/EG anodes

To evaluate the device performances of PEG treated PEDOT:PSS samples, solar cell devices using PEDOT:PSS anodes were fabricated. The chemical structures of the active layer chemicals (P3HT and $PC_{61}BM$) and the device architecture are shown in Fig. 7a and b. The effect of PEG concentration on the device performance was assessed for PEDOT:PSS anodes treated with different molecular weight PEGs and the current density (J)–voltage (V) curves of the devices are shown in Fig. S3 (ESI†), and the power conversion efficiency (PCE), short-circuit current density (J_{SC}), open-circuit voltage (V_{OC}) and fill factor (FF)

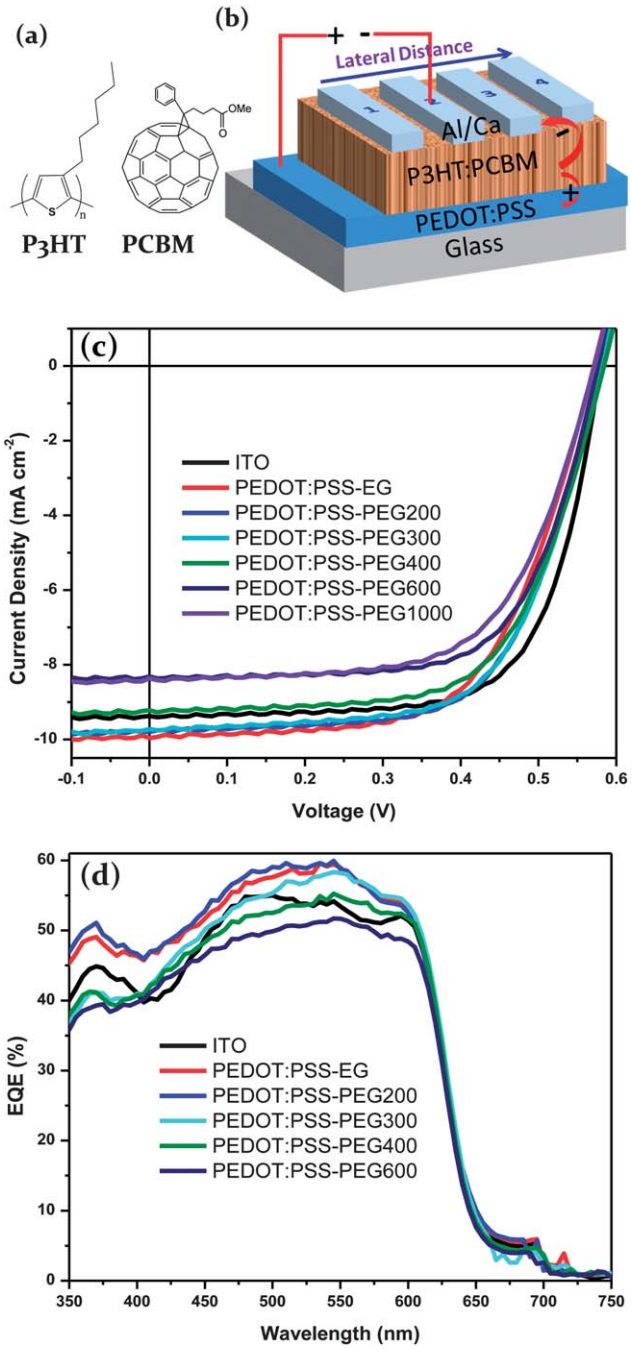

Fig. 7 (a) Chemical structures of active layer chemicals. (b) Device architecture of the ITO-free OSC. (c) *J–V* curves of OSCs with ITO and PEDOT:PSS treated with 6% EG and 2% PEG anodes. (d) EQE spectra of OSCs with ITO and PEDOT:PSS treated with 6% EG and 2% PEG anodes.

values extracted from the *J–V* curves are given in Tables S1–S3 (ESI†). The PCE increased from 1% to 2% PEG200 concentration and then decreased gradually but the minimum PCE is more than 3.12% for 6% PEG200 (Table S1, ESI†). For PEG300 and 400, the PCE is maximum at 2% PEG concentration and then decreased rapidly, the PCE being 1.62% for 6% PEG300 and 1.37% for 6% PEG400. The same trend is observed for PEG600 and 1000 (not shown here). In all cases, the decrease in

Table 1 Photovoltaic performances of OSCs with ITO and PEDOT:PSS treated with 6% EG and 2% PEG anodes extracted from *J–V* curves

Anode	J_{SC} (mA cm^{-2})	V_{OC} (V)	FF (%)	PCE (%)
ITO	9.38	0.58	68.56	3.73
PEDOT:PSS–EG	9.85	0.58	61.44	3.51
PEDOT:PSS–PEG200	9.80	0.58	63.69	3.62
PEDOT:PSS–PEG300	9.73	0.58	63.61	3.59
PEDOT:PSS–PEG400	9.22	0.58	64.14	3.43
PEDOT:PSS–PEG600	8.32	0.58	66.11	3.19
PEDOT:PSS–PEG1000	8.37	0.58	62.21	3.02

PCE with increasing PEG concentration is due to the decrease in J_{SC}. The reason for the rapid decrease in J_{SC} should not be conductivity as the conductivity only changes slightly from 2% to 6% PEG concentration. The reason should be the presence of a thin layer of insulator PEG on the PEDOT:PSS film. In the case of PEG200, nil or negligible amount of PEG is present in the PEDOT:PSS film (as can be seen from the XPS spectra) and this should be well mixed with PEDOT:PSS and hence the J_{SC} does not decrease rapidly with increasing PEG concentration.

Fig. 7c and d show the *J–V* curves and EQE spectra of the OSCs with PEDOT:PSS treated with 2% PEG anodes. OSCs using ITO with less conductive PEDOT:PSS (Clevios P VP Al 4083) buffer layer and PEDOT:PSS treated with 6% EG anodes were also fabricated as control devices. The PCE, J_{SC}, V_{OC} and FF values extracted from the *J–V* curves of the OSCs are given in Table 1. Generally, PEDOT:PSS anodes treated with EG and PEG200 and PEG300 showed higher J_{SC} values than the ITO anode owing to their high transmittance. The PEDOT:PSS anode treated with 2% PEG200 showed a J_{SC} of 9.8 mA cm^{-2}, a V_{OC} of 0.58 V and a PCE of 3.62% with a FF of 63.69%. The device with the reference ITO electrode has a PCE of 3.73% with a little higher FF of 68.56% and a lower J_{SC} of 9.38 mA cm^{-2}. PEDOT:PSS treated with 6% EG has lower performance compared to PEG200 and 300 due to lower conductivity and higher sheet resistance. The lower PCE and J_{SC} of PEDOT:PSS anodes treated with 2% PEG400 are attributed to the presence of PEG in the film as the film conductivity and transmittance are comparable to those of PEG200 and 300. Interestingly, all PEDOT:PSS electrodes showed the same V_{OC} value as that of the ITO counterpart and their FF is higher than 61%. The EQE values are in agreement with the *J–V* values of the devices. For PEDOT:PSS electrodes, there is usually power loss along the lateral distance (shown in Fig. 7b) due to high sheet resistance which decreases the FF.[58] Since our PEG treated PEDOT:PSS electrodes have lower sheet resistance, the FF was falling from ~64% for the first finger to only 58% for the fourth finger. This fall was further decreased without affecting the PCE by using multiple layer PEDOT:PSS anodes.

4 Conclusions

In conclusion, we have shown that the molecular weight of additives affect the degree of conductivity enhancement of PEDOT:PSS. The conductivity of PEDOT:PSS was enhanced to 805 S cm^{-1} with 2% PEG200, 300 and 400 while to only 640 S

cm^{-1} with 6% EG. The increase in carrier concentration by three orders of magnitude after the PEG and EG treatments is the main reason for the conductivity enhancement. PEG treated films also have transmittances as high as 93%. The mechanism of conductivity enhancement is similar to EG. FTIR and XPS measurements showed that PEG remains in the film. PEG and EG give screening between coulombically attracted PEDOT and PSS and lead to phase separation and reorientation of the PEDOT chains and bigger particle aggregates. For PEGs with molecular weights above 400, the mobility of the PEG chains is less and hence conductivity enhancement by PEG is less. PEG forms hydrogen bonding with hygroscopic PSS and enhances the conductivity stability. The presence of PEG on the film surface affects the OSC device performance and 2% PEG concentration gave the best efficiency for all molecular weight PEGs. OSC devices with PEG treated anodes showed a PCE of 3.62%, while those treated with EG showed 3.51% and the ITO counterpart showed 3.73%. Our work clarifies the mechanism of conductivity enhancement associated with the additives in PEDOT:PSS films.

Acknowledgements

This work was financially supported by the Thematic Project of Academia Sinica (AS-100-TP-A05), and the National Science Counsel (NSC 101-2221-E-001-010), Taiwan.

Notes and references

1 B. Azzopardi, C. J. M. Emmott, A. Urbina, F. C. Krebs, J. Mutale and J. Nelson, *Energy Environ. Sci.*, 2011, **4**, 3741.
2 N. Espinosa, M. Hosel, D. Angmo and F. C. Krebs, *Energy Environ. Sci.*, 2012, **5**, 5117.
3 R. Søndergaard, M. Hösel, D. Angmo, T. T. Larsen-Olsen and F. C. Krebs, *Mater. Today*, 2012, **15**, 36.
4 NREL, Best research cell efficiencies, http://www.nrel.gov/ncpv/images/efficiency_chart.jpg, accessed April 12, 2013.
5 J. You, L. Dou, K. Yoshimura, T. Kato, K. Ohya, T. Moriarty, K. Emery, C.-C. Chen, J. Gao, G. Li and Y. Yang, *Nat. Commun.*, 2013, **4**, 1446.
6 L. Dou, J. You, J. Yang, C.-C. Chen, Y. He, S. Murase, T. Moriarty, K. Emery, G. Li and Y. Yang, *Nat. Photonics*, 2012, **6**, 180.
7 C. S. Tao, J. Jiang and M. Tao, *Sol. Energy Mater. Sol. Cells*, 2011, **95**, 3176.
8 A. Chipman, *Nature*, 2007, **449**, 131.
9 J. Cui, A. Wang, N. L. Edleman, J. Ni, P. Lee, N. R. Armstrong and T. J. Marks, *Adv. Mater.*, 2001, **13**, 1476.
10 C. J. M. Emmott, A. Urbina and J. Nelson, *Sol. Energy Mater. Sol. Cells*, 2012, **97**, 14.
11 R. Zhu, C.-H. Chung, K. C. Cha, W. Yang, Y. B. Zheng, H. Zhou, T.-B. Song, C.-C. Chen, P. S. Weiss, G. Li and Y. Yang, *ACS Nano*, 2011, **5**, 9877.
12 J.-Y. Lee, S. T. Connor, Y. Cui and P. Peumans, *Nano Lett.*, 2008, **8**, 689.
13 M.-G. Kang, M.-S. Kim, J. Kim and L. J. Guo, *Adv. Mater.*, 2008, **20**, 4408.
14 K.-H. Tu, S.-S. Li, W.-C. Li, D.-Y. Wang, J.-R. Yang and C.-W. Chen, *Energy Environ. Sci.*, 2011, **4**, 3521.
15 Z. Wu, Z. Chen, X. Du, J. M. Logan, J. Sippel, M. Nikolou, K. Kamaras, J. R. Reynolds, D. B. Tanner, A. F. Hebard and A. G. Rinzler, *Science*, 2004, **305**, 1273.
16 G. Gruner, *J. Mater. Chem.*, 2006, **16**, 3533.
17 L. Gomez De Arco, Y. Zhang, C. W. Schlenker, K. Ryu, M. E. Thompson and C. Zhou, *ACS Nano*, 2010, **4**, 2865.
18 S. Bae, H. Kim, Y. Lee, X. Xu, J.-S. Park, Y. Zheng, J. Balakrishnan, T. Lei, H. Ri Kim, Y. I. Song, Y.-J. Kim, K. S. Kim, B. Ozyilmaz, J.-H. Ahn, B. H. Hong and S. Iijima, *Nat. Nanotechnol.*, 2010, **5**, 574.
19 K. S. Kim, Y. Zhao, H. Jang, S. Y. Lee, J. M. Kim, K. S. Kim, J.-H. Ahn, P. Kim, J.-Y. Choi and B. H. Hong, *Nature*, 2009, **457**, 706.
20 G. Gustafsson, Y. Cao, G. M. Treacy, F. Klavetter, N. Colaneri and A. J. Heeger, *Nature*, 1992, **357**, 477.
21 F. Zhang, M. Johansson, M. R. Andersson, J. C. Hummelen and O. Inganäs, *Adv. Mater.*, 2002, **14**, 662.
22 Y. Xia, K. Sun and J. Ouyang, *Energy Environ. Sci.*, 2012, **5**, 5325.
23 J. Ouyang, C. W. Chu, F. C. Chen, Q. Xu and Y. Yang, *Adv. Funct. Mater.*, 2005, **15**, 203.
24 H. Yan, T. Jo and H. Okuzaki, *Polym. J.*, 2011, **43**, 662.
25 L. Groenendaal, F. Jonas, D. Freitag, H. Pielartzik and J. R. Reynolds, *Adv. Mater.*, 2000, **12**, 481.
26 S. Kirchmeyer and K. Reuter, *J. Mater. Chem.*, 2005, **15**, 2077.
27 H.-Y. Wei, J.-H. Huang, C.-Y. Hsu, F.-C. Chang, K.-C. Ho and C.-W. Chu, *Energy Environ. Sci.*, 2013, **6**, 1192.
28 R. Po, C. Carbonera, A. Bernardi, F. Tinti and N. Camaioni, *Sol. Energy Mater. Sol. Cells*, 2012, **100**, 97.
29 J.-H. Huang, D. Kekuda, C.-W. Chu and K.-C. Ho, *J. Mater. Chem.*, 2009, **19**, 3704.
30 J. Huang, P. F. Miller, J. S. Wilson, A. J. de Mello, J. C. de Mello and D. D. C. Bradley, *Adv. Funct. Mater.*, 2005, **15**, 290.
31 A. M. Nardes, M. Kemerink, M. M. de Kok, E. Vinken, K. Maturova and R. A. J. Janssen, *Org. Electron.*, 2008, **9**, 727.
32 Y. Zhou, H. Cheun, S. Choi, J. W. J. Potscavage, C. Fuentes-Hernandez and B. Kippelen, *Appl. Phys. Lett.*, 2010, **97**, 153304.
33 M. Reyes-Reyes, I. Cruz-Cruz and R. n. López-Sandoval, *J. Phys. Chem. C*, 2010, **114**, 20220.
34 C. Badre, L. Marquant, A. M. Alsayed and L. A. Hough, *Adv. Funct. Mater.*, 2012, **22**, 2723.
35 C.-J. Ko, Y.-K. Lin, F.-C. Chen and C.-W. Chu, *Appl. Phys. Lett.*, 2007, **90**, 063509.
36 Y. J. Xia, H. M. Zhang and J. Y. Ouyang, *J. Mater. Chem.*, 2010, **20**, 9740.
37 Y. Xia and J. Ouyang, *Org. Electron.*, 2010, **11**, 1129.
38 Y. Xia and J. Ouyang, *ACS Appl. Mater. Interfaces*, 2010, **2**, 474.
39 Y. Xia, H. Zhang and J. Ouyang, *J. Mater. Chem.*, 2010, **20**, 9740.
40 Y. Xia and J. Ouyang, *J. Mater. Chem.*, 2011, **21**, 4927.
41 Y. H. Kim, C. Sachse, M. L. Machala, C. May, L. Müller-Meskamp and K. Leo, *Adv. Funct. Mater.*, 2011, **21**, 1076.
42 Y. Xia, K. Sun and J. Ouyang, *Adv. Mater.*, 2012, **24**, 2436.

43 M. V. Fabretto, D. R. Evans, M. Mueller, K. Zuber, P. Hojati-Talemi, R. D. Short, G. G. Wallace and P. J. Murphy, *Chem. Mater.*, 2012, **24**, 3998.
44 S.-I. Na, G. Wang, S.-S. Kim, T.-W. Kim, S.-H. Oh, B.-K. Yu, T. Lee and D.-Y. Kim, *J. Mater. Chem.*, 2009, **19**, 9045.
45 J. Ouyang, Q. Xu, C.-W. Chu, Y. Yang, G. Li and J. Shinar, *Polymer*, 2004, **45**, 8443.
46 D. Alemu, H.-Y. Wei, K.-C. Ho and C.-W. Chu, *Energy Environ. Sci.*, 2012, **5**, 9662.
47 S.-I. Na, S.-S. Kim, J. Jo and D.-Y. Kim, *Adv. Mater.*, 2008, **20**, 4061.
48 J. Y. Kim, J. H. Jung, D. E. Lee and J. Joo, *Synth. Met.*, 2002, **126**, 311.
49 T. Takano, H. Masunaga, A. Fujiwara, H. Okuzaki and T. Sasaki, *Macromolecules*, 2012, **45**, 3859.
50 T. Wang, Y. Qi, J. Xu, X. Hu and P. Chen, *Appl. Surf. Sci.*, 2005, **250**, 188.
51 C. Kittle, *Introduction to Solid State Physics*, John Wiley & Sons, Inc., 2005.
52 J. Ouyang, C. W. Chu, F. C. Chen, Q. Xu and Y. Yang, *J. Macromol. Sci., Part A: Pure Appl.Chem.*, 2004, **41**, 1497.
53 X. Crispin, F. L. E. Jakobsson, A. Crispin, P. C. M. Grim, P. Andersson, A. Volodin, C. van Haesendonck, M. Van der Auweraer, W. R. Salaneck and M. Berggren, *Chem. Mater.*, 2006, **18**, 4354.
54 T. P. Nguyen and S. A. de Vos, *Appl. Surf. Sci.*, 2004, **221**, 330.
55 Y. Xia and J. Ouyang, *ACS Appl. Mater. Interfaces*, 2012, **4**, 4131.
56 A. Aleshin, R. Kiebooms, R. Menon and A. J. Heeger, *Synth. Met.*, 1997, **90**, 61.
57 U. Lang, E. Müller, N. Naujoks and J. Dual, *Adv. Funct. Mater.*, 2009, **19**, 1215.
58 M. W. Rowell, M. A. Topinka, M. D. McGehee, H.-J. Prall, G. Dennler, N. S. Sariciftci, L. Hu and G. Gruner, *Appl. Phys. Lett.*, 2006, **88**, 233506.